

Diseño y simulación de un sistema de generación fotovoltaica para una cocina de inducción

Design and simulation of a photovoltaic generation system for an induction cooker

Projeto e simulação de um sistema de geração fotovoltaica para um fogão de indução

Rita Paola León Pérez

Universidad de las Fuerzas Armadas-ESPE, Ecuador

rpleon1@espe.edu.ec

Darwin Leónidas Aguilar Salazar

Universidad de las Fuerzas Armadas-ESPE, Ecuador

dlaguilar@espe.edu.ec

Rubén David Vélez Ortuño

Universidad de las Fuerzas Armadas-ESPE, Ecuador

rdvelez@espe.edu.ec

Diego Gustavo Arcos Avilés

Universidad de las Fuerzas Armadas-ESPE, Ecuador

dgarcos@espe.edu.ec

Resumen

El presente proyecto consiste en diseñar y simular los elementos necesarios para las etapas que conforman un sistema de generación fotovoltaica que permitE abastecer de energía a una cocina de inducción magnética. Para ello se muestran los procedimientos de diseño de las etapas de potencia, almacenamiento y generación fotovoltaica, las cuales conforman cada uno de los sistemas de generación fotovoltaica, uno sin sistema de almacenamiento y dos con

sistema de almacenamiento. La simulación de cada uno de los modelos planteados se desarrolla con el software Matlab-Simulink, las etapas de potencia se desarrollan con la librería SimPowerSystems, el diseño de los controladores se desarrolla con la librería Sisotool, y el desarrollo de las simulaciones se comprueba con el correcto funcionamiento de los sistemas dentro de los parámetros establecidos. Finalmente se comparan los modelos desarrollados a fin de determinar cuál es el sistema más propicio para abastecer de energía a la cocina de inducción magnética.

Palabras clave: sistemas fotovoltaicos, sistemas de potencia, cocina de inducción, control PID, paneles fotovoltaicos.

Abstract

In this project presents the design and simulation of the elements necessary to design the stages that are part of a photovoltaic generation system that allows power supply to a magnetic induction cooker. Showing design procedures of the power stages, storage and photovoltaic generation, for each photovoltaic generation systems, for this the following models were defined: a model for a photovoltaic system without storage system, and two models for photovoltaic system with storage system. The simulation of each of the proposed models was made in the software Matlab - Simulink, the power stages are developed by SimPowerSystems library, the design of controllers developed by Sisotool library. Through simulations it checked the correct functioning of the systems under the established parameters. Additionally the models developed to determine what is the most suitable for the supply of energy for cooking magnetic induction system is compared.

Key words: photovoltaic systems, power systems, induction cooker, PID control photovoltaic panels.

Resumo

Este projeto é projetar e simular os elementos necessários para as fases que compõem um sistema de geração de energia fotovoltaica que permite fornecimento de energia a um fogão de indução magnética. Para estes procedimentos de design das fases de energia, armazenamento e geração fotovoltaica são mostrados, que formam cada sistemas de geração fotovoltaica, um sem sistema de armazenamento e dois sistema de armazenamento. A

simulação de cada um dos modelos propostos é desenvolvido com software Matlab-Simulink, as fases de energia são desenvolvidos com a biblioteca SimPowerSystems, o projeto do controlador é desenvolvido com a biblioteca Sisotool, e desenvolvimento de simulações é verificada o bom funcionamento dos sistemas dentro dos parâmetros estabelecidos. Finalmente, os modelos desenvolvidos para determinar o que é o mais propício para fornecer energia para o sistema de cozimento por indução magnética são comparados.

Palavras-chave: sistemas fotovoltaicos, sistemas de energia, fogão de indução, controle PID, painéis fotovoltaicos.

Fecha recepción: Septiembre 2015

Fecha aceptación: Enero 2016

Introduction

The use of renewable energy for generating electric energy is becoming more popular as it seeks to respect nature and stop relying on fossil resources. The Ecuadorian State promotes the use of renewable resources such as water, wind and sun to generate energy; several wind, hydroelectric and solar projects are developed in the country with the view of changing the energy matrix that seeks to stop dependence on non-renewable resources in energy generation. Among the changes involved in the energy matrix is the replacement of Liquefied Petroleum Gas (LPG) as a source for electric power generation in household kitchens. The Ecuadorian government supports projects involving the use of renewable energy, and thus raises the inclusion of a photovoltaic generation system for an induction cooker magnética.

A photovoltaic generation system is a set of devices that work together to generate electricity based on solar radiation available at certain times of day, from that conditioning the inclusion of a storage system to photovoltaic generation system arises for have electricity and stop depending on the weather situation. This requires a photovoltaic generation system and non-system energy storage arises, analysis of the power stages (conversion and investment),

storage system and photovoltaic generation system, is performed controllers are designed and finally, the results obtained for the simulations the proposed designs are presented.

Design Considerations

The design conditions used in this study are as follows:

Simplified model of the photodetector

The simplified model of the photodetector is determined by considering that there are no power losses in the energy transformation process (Figure 1).

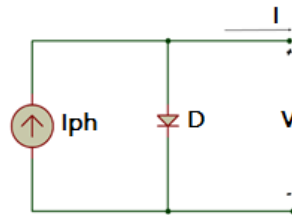


Figure 1. Modelo de Célula Fotoeléctrica.

General model of the photovoltaic cell

This circuit considers losses in the process by including the resistance in the circuit (Figure 2).

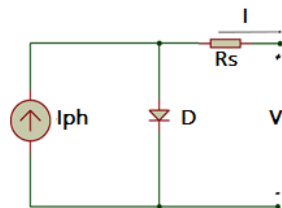


Figure 2. Modelo general de la célula fotoeléctrica.

General model of the photovoltaic module

The circuit consists of n number of cells in series and n Ns number of cells in parallel Np, a photocell and a resistor Rs (Figure 3) series.

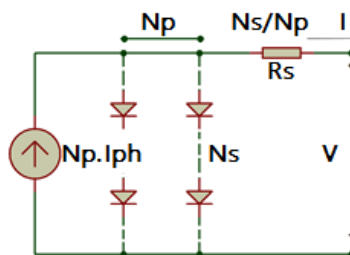


Figure 3. Modelo general de módulo fotoeléctrico.

For the design of the photovoltaic generator module ISOFOTON I165 model, whose electrical characteristics for a single module mark is presented in Table was used.

Table I. Características eléctricas Isofoton I165

No.	Marca	Modelo	Potencia (W)	I _{mpp} (A)	V _{mpp} (V)	I _{sc} (A)	V _{oc} (V)
1	Isofoton	I165	165	9.48	17.4	10.06	21.6

Power converters

DC-DC boost converter

It is a power device that provides at its output a voltage higher than the input voltage, $V_o > V_i$ [11] figure 4.

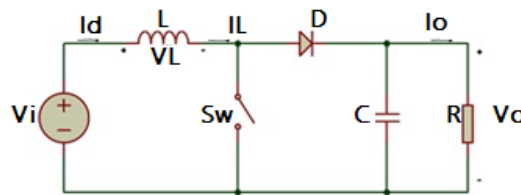


Figure 4. Convertidor elevador DC-DC

The transfer function of the boost converter is defined based on the analysis in steady state and dynamic state (1).

$$G(s) = \frac{V_o}{1-D} \frac{1 - \frac{Ls}{(1-D)^2 \times R}}{LCs^2 + \frac{Ls}{(1-D)^2} + \frac{Ls}{(1-D)^2 \times R} + 1} \tag{1}$$

DC-DC buck converter

It is a power device that provides at its output an average value V or lower voltage to the input voltage V_i (figure 5).

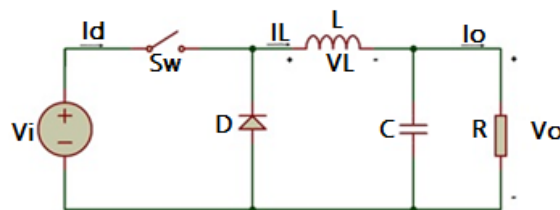


Figure 5. Convertidor reductor DC-DC.

Equations (2) and (3) allow calculating the values of the inductance and capacitance of the converter.

$$L = \frac{V_o}{\Delta i_L \cdot f} \tag{2}$$

$$C = \frac{I_o \cdot D}{\Delta V_o \cdot f} \tag{3}$$

Where: L inductancia, C capacitancia, f frecuencia, ΔV_o variación de voltaje y Δi_L variación de corriente en inductor. In step (4) the transfer function is shown, calculated based on equations of state of the buck converter.

$$\frac{V_{out}(s)}{D(s)} = \frac{\frac{1}{LC}}{\left[s^2 + \frac{1}{RC} s + \frac{1}{LC} \right]} \tag{4}$$

DC-AC inverter and filter

The DC-AC converters are switching circuits that generate electric power by alternating current from a source⁵⁻⁶. The topology of the full bridge type inverter and LC filter is shown in Figure 6.

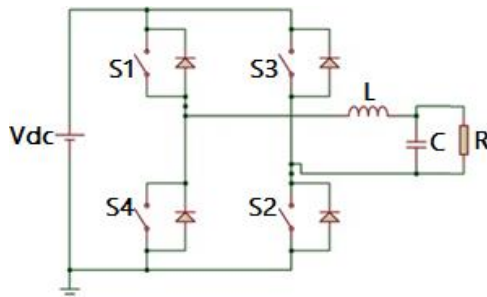


Figure 6. Inversor DC-AC y Filtro LC.

The transfer function relating the inverter output voltage variation of pulses that control switches the inverter (5).

$$\frac{V_o(s)}{m(s)} = \frac{V_{DC} \times R}{s^2 RCL + s(LRCR_L) + R + R_L} \tag{5}$$

Energy storage system

A commercial bank whose electrical characteristics are presented in Table 7 was used to obtain the technical characteristics and determine the number of batteries needed for the system.

Table II. Características eléctricas ULTRACELL modelo UCG 150-12

Voltaje nominal	12V
Capacidad nominal	150Ah
Características de Capacidad	160.8Ah/8.04A (20hrs,1.8V/cell, 25 ⁰ C)
	150Ah/15.0A (10hrs,1.8V/cell, 25 ⁰ C)
	131.6Ah/26.3A (5hrs,1.8V/cell, 25 ⁰ C)

By (6) the ability of the storage system is calculated and (7) calculates the number of batteries that must contain the storage system.

$$C_{bat} = \frac{D_{total} \times Aut}{V_{bat} \times DOD} \tag{6}$$

$$NúmeroBaterias = \frac{C_{bat}}{C_{carga}} \tag{7}$$

Where: C_{bat} capacidad de una batería, Aut autonomía de un sistema de almacenamiento, V_{bat} voltaje en una batería, DOD factor de eficiencia del sistema de almacenamiento y C_{carga} capacidad requerida por el sistema.

Initial considerations

- The induction cooker will have a maximum power of 1300 watts, supplied with a voltage of 120 V and 60 Hz frequency, device consumes 21.6 A.
- Daily use of the kitchen is limited to 2 hours 45 minutes a day.
- The geographical location for which the analysis is to be conducted Quito-Ecuador.
- In designing the photovoltaic system with storage system without the same business model of photovoltaic module and battery used.
- In the photovoltaic system with storage system, it will be estimated autonomy time of 1 day.
- To simulate the same design DC-AC inverter for systems with and without energy storage is used.

- The sizing of the storage system will be equal to the first and second fotovoltaico1 model system.

Load analysis and solar radiation

Load analysis

The induction cooker is considered a cyclical load, use 2 hours 45 minutes a day, a value of 3600 kWh / day, and 10% safety margin, which power consumption is obtained (8).

$$D_{total} = \frac{(Ddiaria*10\%)+Ddiaria}{factor\ de\ unidades} = 3.96 \frac{kwh}{dia}$$

$$D_{total} = \frac{(3600 * 0.1) + 3600}{1000} = 3.96 \frac{kwh}{dia} \tag{8}$$

Solar radiation

Solar radiation available for the city of Quito is consulted in the "Solar Atlas of Ecuador purposes Electricity Generation" published by the CONECEL [10]. The values used for design are those with the worst conditions during the year, whose value is 4800Wh/m2/día.

Design and simulation of the PV system without storage system

This system consists of devices: arrangement of photovoltaic modules, DC-DC boost converter, DC-AC inverter and filter. The configuration of this model is presented in Figure 7

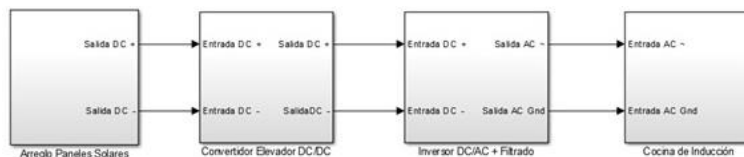


Figura 7. Topología sistema fotovoltaico sin sistema de almacenamiento.

Design panel arrangement

Considering a yield of 90% for the system is given by (9) the total of 9 units of photovoltaic panels which are divided into three modules connected in parallel, with three modules connected in series and with a total power of 1485 W.

$$N_{\text{paneles}} = \frac{D_{\text{total}}}{P_{\text{mpp}} \times \text{HSP} \times F_g} \tag{9}$$

Where: D_{total} demanda total [wh/dia], P_{mpp} punto de máxima potencia, HSP radiación solar disponible y F_g rendimiento del panel solar.

Power Converters

DC-DC boost converter

Designing the upconverter is considered: $V_o=200\text{v}$; $V_i=52\text{v}$; $f=20\text{Khz}$; maximum ripple current 10%; ripple voltage maximum 1% of the output voltage, whereby the values of inductance and capacitance will: $L=829 \text{ uH}$ y $C= 200\text{uF}$.

Figure 8 shows simulation upconverter shown, on top the output current of the boost converter and the input current generated by the panel arrangement shown, while at the bottom the output voltage shown boost converter and the output voltage. It can be seen that at $t = 0.35 \text{ s}$ the converter reaches its steady state with a value of 200V.

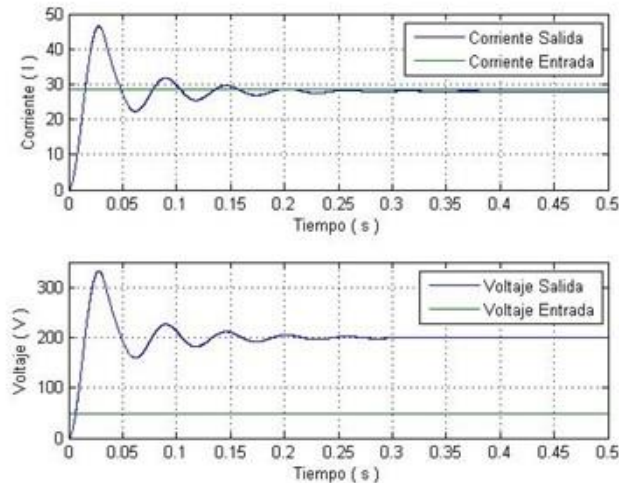


Figure 8. Simulación del convertidor elevador del sistema fotovoltaico sin sistema de almacenamiento.

DC-AC inverter

To design the investor considers the following:

- The inverter input voltage is the voltage delivered by the upconverter (200 V).
- The output voltage of the investment process and filtering V_o is 120 Vrms.
- Modulator: $f_{mod} = 60\text{Hz}$ frequency and peak amplitude of the control signal $v_c = 200 \text{ V}_p$.
- Carrier: frequency $f_s = 6\text{KHz}$ and peak amplitude of the control signal $v_{tri} = 240 \text{ V}_p$.
- Technical Modulation method sinusoidal pulse width modulated unipolar SPWM.
- Stage filtering: LC lowpass filter type.

In Figure 9, the voltage signal and output current of the inverter with filtering stage shows, and observed that the signals are sinusoidal with a frequency of 60 Hz and an amplitude of 170 Vpeak, 120 Vrms.

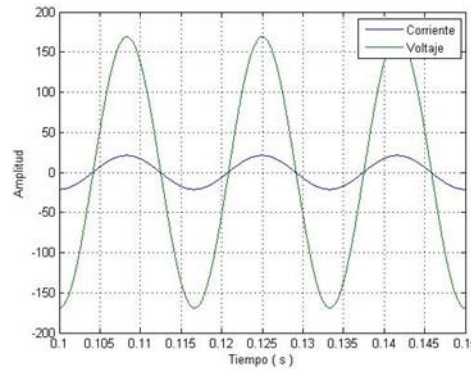


Figure 9. Simulación del inversor con etapa de filtrado del sistema fotovoltaico sin sistema de almacenamiento.

Design system drivers

Photovoltaic system controllers were designed without storage system for power amplifiers elevator DC / DC converter, inverter DC / AC and filter. By replacing the inductor and capacitor values and duty cycle D , it is the floor of the boost converter and the inverter (10) and (11) respectively.

$$G_p(s) = \frac{-0.07974 s + 200}{6.13 \times 10^{-6} s^2 + 0.0003987 s + 1} \tag{10}$$

$$G_p(s) = \frac{120}{2.80 \times 10^{-8} s^2 + 1.80 \times 10^{-5} s + 1.07} \tag{11}$$

Using the transfer functions (10) and (11), using the second method of Ziegler-Nichols tuning controllers for PID⁹, the critical gain is calculated K_{cr} , values are determined K_p and T_i , It is

replaced (12) and the controller is. The transfer functions upconverter controller and inverter are presented in equations (13) and (14) respectively.

$$G_c(s) = \frac{K_p \cdot s + \frac{K_p}{T_i}}{s} \tag{12}$$

$$G_c(s) = \frac{3.97 \times 10^{-4} s + 1.199}{s} \tag{13}$$

$$G_c(s) = \frac{3.285 s^2 + 2.475 \times 10^4 s + 1.644 \times 10^7}{s^2 + 1.786 \times 10^5 s} \tag{14}$$

The block diagram of Figures 12 and 13 represent the closed loop systems $G_p(s)$ in series with the PID plant controller $G_c(s)$, with unity feedback, the upconverter and inverter respectively.

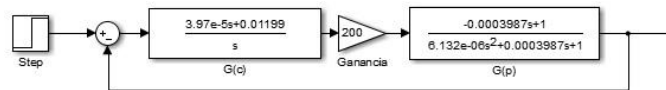


Figure 1. Diagrama de Bloques Controlador PI y Planta, para convertidor elevador de 52 V a 200 V.

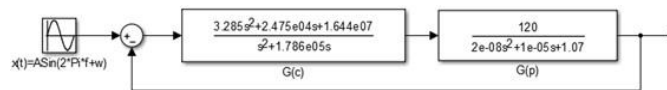


Figure 2. Diagrama de Bloques Controlador PID G(c) y Planta G (p), para inversor 200 VDC a 120 VAC.

Figure 4 shows the variation of solar radiation, which shows that compared to the different variations of radiation controller stabilizes the voltage signal from the upconverter to reach a stable value 200V.

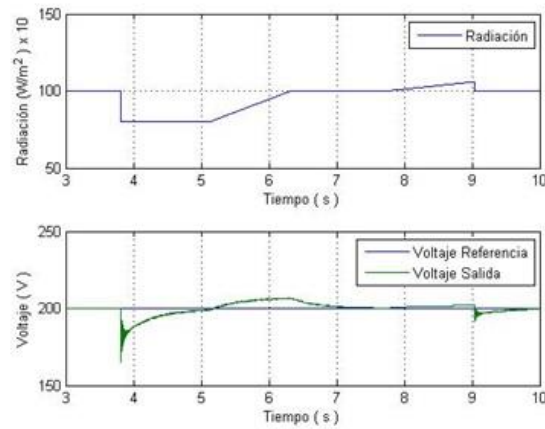


Figure 34. Simulación del Convertidor Elevador del sistema fotovoltaico sin sistema de almacenamiento, frente variación de radiación solar.

In Figure 5 it shows that compared to a voltage variation, the controller stabilizes the voltage signal output of the inverter to reach a stable valuee 170Vpico.

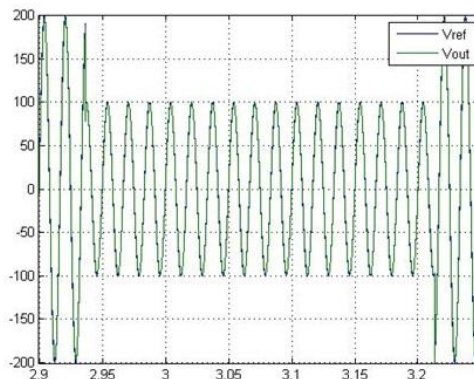


Figure 45. Simulación del inversor del sistema fotovoltaico sin sistema de almacenamiento, frente variación de voltaje en convertidor elevador.

Design and simulation of the photovoltaic system with storage system

This section presents two models of photovoltaic system, which have the following elements were analyzed: arrangement of photovoltaic modules, boost converter DC-DC buck converter hoist DC-DC, DC-AC inverter, filter and storage system, however differ in performance due to:

- First model will be considered as the arrangement of modules deliver the energy generated to the storage system consisting of batteries and charging make use of this energy only.

- Second model is considered that both the arrangement of modules and storage system deliver the power required by the load.

Photovoltaic system with storage system, first model.

The configuration of this model is presented in Figure 16.

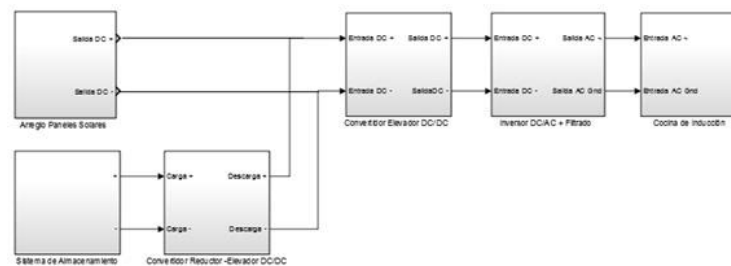


Figure 56. Diagrama de bloques del sistema fotovoltaico con sistema de almacenamiento, primer modelo.

Design panel arrangement

The distribution of the modules is in parallel with three modules connected in series and a total power of 646 W.

Storage System Design

Since the load consumes 21.6 A (design conditions), the battery has chosen $C_{bat} = 131.6\text{Ah}$ (Table 2), then a battery can provide the current for the system by the time mentioned, so you should size the supply system for a period of autonomy for 1 day. The calculation is performed by (6) by substituting the values obtained in the analysis of load (8), maximum rate of discharge of 70% system capacity 472 Ah storage is obtained.

The number of batteries is calculated by (7), the distribution of free storage system is 4 batteries connected in parallel with a $C = 472\text{Ah}$, rated voltage capacity $V_{bat} = 12\text{V}$, which cater for 20 continuous hours to consume a current $I_{BAT} = 26.3\text{A}$.

The storage system has a total discharge rate after 22 hours, as shown in Figure 17. The charging of the storage system will be in a period of 12.44 hours, as seen in Figure 18.

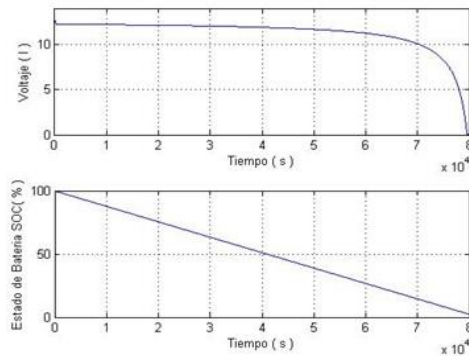


Figure 67. Estado de descarga del sistema de almacenamiento.

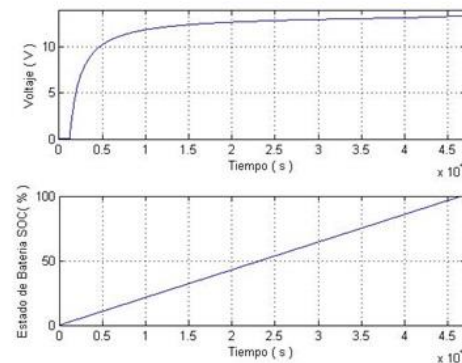


Figure 78. Estado de carga del sistema de almacenamiento.

Design power converters

Design DC-DC boost converter is performed by the following considerations: $V_o = 200\text{ V}$; $V_i = 120\text{ V}$; $f = 20\text{ Khz}$; maximum ripple current 10% of the output current; ripple voltage maximum 1% of the output voltage. As the values of inductance and capacitance are obtained 900 μH y 1000 μF respectively.

Figure 19 shows simulation upconverter, and at the top of the figure the output current of the boost converter and the input current generated by the buck-boost converter is shown, while in the lower voltage shown upconverter output and the input voltage, and it is observed that in $t = 0.2\text{ s}$, el convertidor alcanza el valor de 200V.

For the design of the converter buck-boost the following consideration is made: $V_o = 120\text{ V}$; $V_i = 17\text{ V}$; $f = 20\text{ Khz}$; maximum ripple current 10% of the output current; ripple voltage maximum 1% of the output voltage, whereby the inductance and capacitance will be 290 μH and 500 μF respectively.

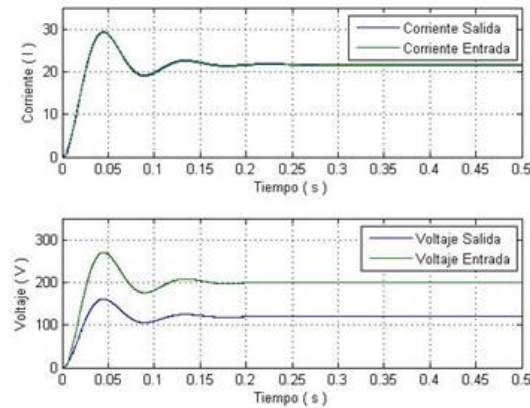


Figure 89. Simulación del convertidor elevador del sistema fotovoltaico con sistema de almacenamiento, primer modelo.

Design system drivers

Similarly, for the storage system design without plant lifter (15) converter and the converter reducer-lift is obtained (16).

$$Gp(s) = \frac{-0.01625 s + 200}{2.5 \times 10^{-6} s^2 + 8.127 \times 10^{-5} s + 1} \tag{15}$$

$$G(s) = \frac{-0.1131 s + 120}{1.45 \times 10^{-5} s^2 + 0.0009428 s + 1} \tag{16}$$

Also by the second method of Ziegler-Nichols is the transfer function of the controller. In (17) and (18) the boost converter and the converter buck-boost respectively are presented.

$$Gc(s) = \frac{1.717s^2 + 912.6 s + 1.067 \times 10^5}{s^2 + 3.94 \times 10^4 s} \tag{17}$$

$$Gc(p) = \frac{0.0005315 s + 0.03928}{s} \tag{18}$$

The block diagram of Figures 20 and 21 represent the closed loop systems $Gp (s)$ in series with the PID plant controller $Gc (s)$, with unity feedback, the upconverter and inverter respectively.

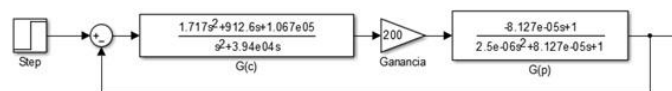


Figure 20. Diagrama de Bloques Controlador PI G(c) y Planta G (p), para convertidor elevador de 120 VDC a 200 VDC.



Figure 21. Diagrama de Bloques Controlador PID G(c) y Planta G(p), convertidor reductor-elevador 17 VDC-120 VDC.

In Figure 22 it can be seen that face the different variations of voltage buck-boost converter, the controller stabilizes the voltage signal from the upconverter to reach stable regime 200V.

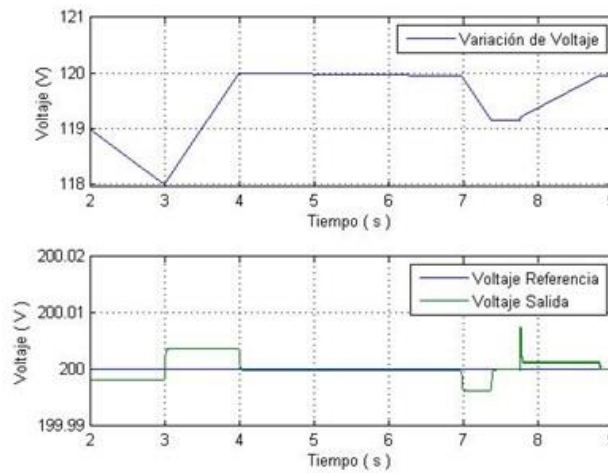


Figure 22. Simulación del Convertidor Elevador del sistema fotovoltaico con sistema de almacenamiento primer modelo, frente variacion de voltaje.

In Figure 23 it can be seen that face the different variations of voltage from the storage system, the controller stabilizes the voltage signal from the buck-boost converter until a stable value 120V.

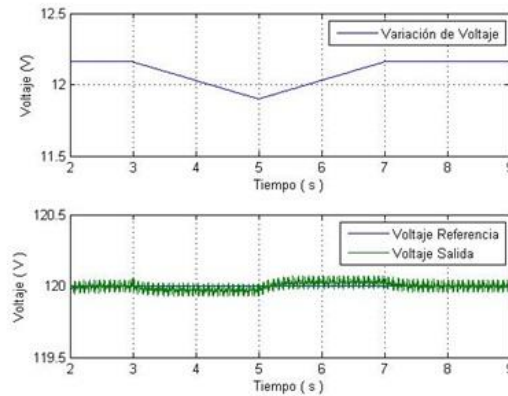


Figure 23. Simulación del convertidor reductor-elevador del sistema fotovoltaico con sistema de almacenamiento primer modelo, frente variacion de voltaje.

Photovoltaic system with storage system, second model.

The configuration of this model is presented in Figure 24.

Design panel arrangement

Under the above conditions a total number of 6 photovoltaic modules is obtained, the distribution of these will be in three modules connected in parallel, with three modules connected in series and a total power of 968 W.

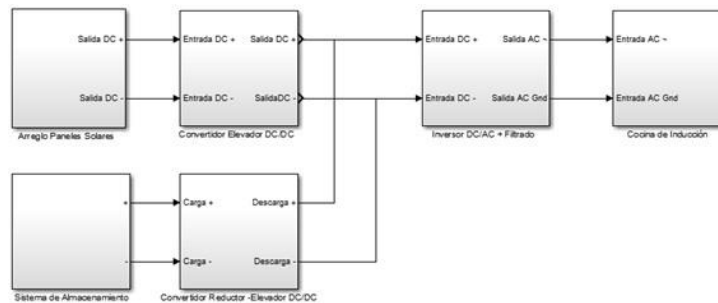


Figure 24. Diagrama de bloques del sistema fotovoltaico con sistema de almacenamiento, segundo modelo.

Design power converters

Design DC-DC boost converter is performed by the following considerations: $V_{o1}=80v$; $V_{i1}=17v$; $V_{o2}=200v$; $V_{i2}=80v$; $f=20Khz$; maximum ripple current 10% of the output current; ripple voltage maximum 1% of the output voltage, being the capacitance and inductance for the two converters connected in cascade, obtaining the following values for the first converter $C=520 \mu F$ y $L=300 \mu H$, and the second converter $C=400 \mu F$ y $L=1090 \mu H$.

Figure 25 shows simulation upconverter cascaded, at the top of the figure the output current of the boost converter and the input current generated by the panel arrangement shown, while the lower part shows the output voltage boost converter and the input voltage generated by the panel arrangement also shows that at $t = 0.1$ s, the drive reaches the value 200.4V. For the design of the converter buck-boost the following consideration is made: $V_o = 200v$; $V_i = 12v$; $f = 20Khz$; maximum ripple current 10% of the output current; ripple voltage maximum 1% of the output voltage, for which capacitance and inductance for the inverter be: $C = 325 \mu F$ and $L = 650 \mu H$.

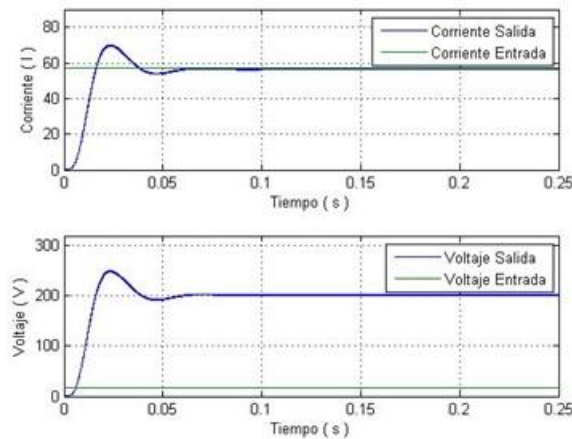


Figure 25. Simulación del Convertidor Elevador del sistema fotovoltaico con sistema de almacenamiento, segundo modelo.

Figure 26 shows the simulation of the buck-boost converter; at the top of the figure the output current of the converter shown in raising step and the input current generated by the storage system, while at the bottom the output voltage of the converter shown in step lifting and input voltage generated by the storage system. The figure shows that in $t = 0.35$ s, converter reductor-elevador alcanza el valor de 200.2V.

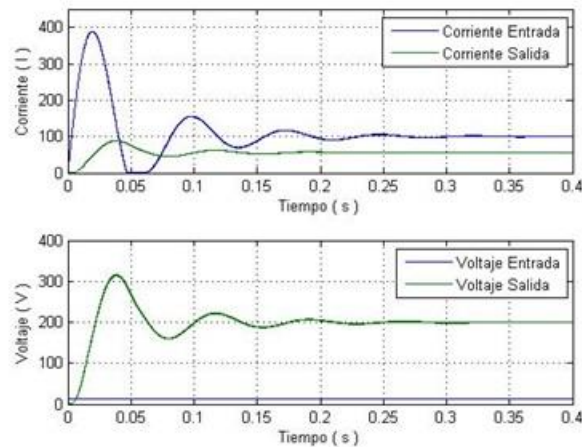


Figure 26. Simulación del Convertidor Reductor - Elevador, Etapa Elevación del sistema fotovoltaico con sistema de almacenamiento, segundo modelo.

Design system drivers

Also plant is upconverter (19), and for reducing upconverter (20).

$$Gp(s) = \frac{-0.108 s + 80}{3.455 \times 10^{-6} s^2 + 0.00135 s + 1} \tag{19}$$

$$Gp(s) = \frac{-1.929 s + 200}{2.924 \times 10^{-5} s^2 + 0.009143 s + 1} \tag{20}$$

Also the transfer functions upconverter controller and buck-boost converter are presented in (21) and (22) respectively.

$$Gc(s) = \frac{0.001622 s + 0.2456}{s} \tag{21}$$

$$Gc(s) = \frac{0.002 s + 0.1041}{s} \tag{22}$$

The block diagram of Figures 27 and 28 represent the closed loop systems $Gp (s)$ in series with the PID plant Gc -reducer elevator controller respectively (s), with unity feedback, and drive the upconverter.



Figure 97. Diagrama de Bloques Controlador PI G(c) y Planta G (p), para convertidor elevador de 17 V a 200 V.

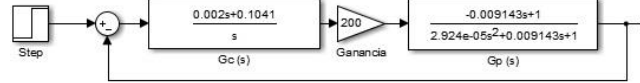


Figure 108. Diagrama de Bloques Controlador PID G(c) y Planta G (p), convertidor reductor-elevador 12 VDC a 200 VAC.

In Figure 29 it can be seen that face the different variations of solar radiation the controller stabilizes the voltage signal from the upconverter to reach a stable value of 200V.

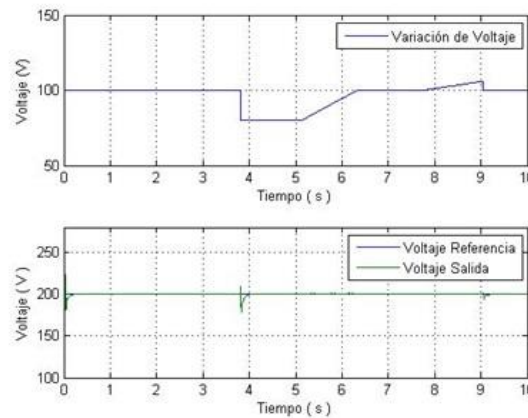


Figure 119. Simulación del Convertidor Elevador, segundo modelo frente variación de radiación solar.

In Figure 30 it can be seen that face the different variations of voltage from the storage system, the controller stabilizes the voltage signal from the buck-boost converter until a stable value of 200V.

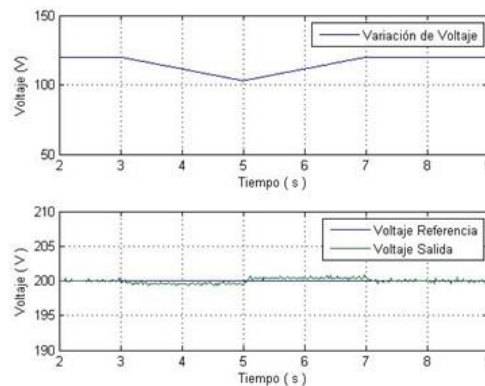


Figure 30. Simulación del Convertidor Reductor - Elevador, Elevación, frente variación de voltaje en sistema de almacenamiento.

Efficiency calculation

The efficiency of the devices that make up each of the designed system is calculated from the beginning of peak performance. For a lossless circuit can be found efficiency by (23) and (24).

$$P_{in} = P_{out} \tag{23}$$

$$n = \frac{P_{out}}{P_{in}} \tag{24}$$

- Photovoltaic system without storage system: Efficiency 89.44 %.

Table III. Eficiencia sistema fotovoltaico sin sistema de almacenamiento

No.	Dispositivo	Potencia Entrada (W)	Potencia Salida (W)	Eficiencia (%)
1	Arreglo de Paneles	No aplica	1375.1308	
2	Convertidor Elevador [52Vdc-200Vdc]	1375.1308	1355.4251	98.567
3	Inversor [200Vdc-120Vac]	1355.4251	1328.1268	97.986

- Photovoltaic system with storage system, first model: Efficiency 85.53 %.

Table IV. Eficiencia sistema fotovoltaico con sistema de almacenamiento, primer modelo.

No.	Dispositivo	Potencia Entrada (W)	Potencia Salida (W)	Eficiencia (%)
1	Arreglo de Paneles	No aplica	1375.130	
2	Convertidor Elevador [52Vdc-200Vdc]	1375.130	1327.589	96.54
3	Inversor [200Vdc-120Vac]	1327.589	1230.011	92.65

- Photovoltaic system with storage system, second model: Efficiency 86.66 %.

Table V. Eficiencia sistema fotovoltaico con sistema de almacenamiento, segundo modelo.

No.	Dispositivo	Potencia Entrada (W)	Potencia Salida (W)	Eficiencia
1	Arreglo de Paneles	No aplica	989.712	
2	Convertidor Reductor-Elevador [12Vdc-200Vdc]	No aplica	975.133	
2	Convertidor Elevador [12Vdc-200Vdc]	989.712	925.776	93.54
3	Inversor [200Vdc-120Vac]	925.776	857.73	92.65

Discussion and conclusions

By analyzing the simulations was verified that the design made for photovoltaic systems with and without storage system meet the proposed parameters. The obtained mathematical models for the power units of each design systems allowed voltage controllers, which have good performance against disturbances applied, achieving stabilized against changes in voltage produced by the array of photovoltaic panels.

The integration of a system based storage batteries in photovoltaic system represents a benefit at any time require power, even if the arrangement does not produce energy photovoltaic panels.

The results obtained by simulations show that the photovoltaic system without storage system has an efficiency of 89.44% increase compared with the two models of photovoltaic system with storage system (86.66%), however, the second model has the advantage of operate at any time of day, so this would be the best choice when making a deployment.

For future work can be considered a two-phase inverter in the adaptation of induction cookers who offer commercial houses in Ecuador and that are within the power generated by the photovoltaic system additionally can make the measurement of parameters of power quality AC, which provide information for possible changes in the design of devices to help improve system performance.

Gratefulness

This study was conducted with the support of the University of the Armed Forces -ESPE by the research project "Design and Simulation of a System-Based Power Generation Photovoltaic Solar Energy with and without Energy Storage System for Kitchen Magnetic Induction".

Bibliography

- A. Abreu (2005). Calidad de Potencia Eléctrica en Redes de Distribución. Venezuela, p. 124.
- A. Hermosa (2011). Electrónica Aplicada. España: Marcombo, S.A, p. 69.
- A. Pozo (2011). Convertidores Conmutados de Potencia. Test de Autoevaluación. Barcelona, España: Marcombo, S.A, p. 214.
- C. Solanski (2011). Solar Photovoltaics: Fundamentals, Technologies and Applications, Second Edi. India: Prentice-Hall, p. 512.
- D. Hart (2001). Electrónica de Potencia. Madrid, España: Pearson Educación, S.A, p. 323.
- G. Garcerá (1998). Conversores conmutados: circuitos de potencia y control. Valencia, España: Camino de Vera, p. 76.
- Izquierdo (2008). “Atlas Solar del Ecuador con fines de Generación Eléctrica” [Online]. Available: http://www.conelec.gob.ec/archivos_articulo/Atlas.pdf
- J. Valentín (2012). Instalaciones Solares Fotovoltaicas. San Sebastián, España: Donostierra, p. 32.
- K. Ogata (2010). Ingeniería de Control Moderna, 5a ed. España, p. 570.
- L. Prat (1999). Circuitos y Dispositivos Electrónicos: Fundamentos de Electrónica. Catalunya, España: Universidad Politécnica de Catalunya, p. 463.
- M. García (1999). Energía Solar Fotovoltaica y Cooperación al Desarrollo. Madrid, España: IEPALA Editorial, p. 62.
- M. H. Rasid (2004). Electrónica de potencia: circuitos, dispositivos y aplicaciones, Third Edit. Mexico: Pearson Educación, p. 33.
- M. Pareja (2010). Energía Solar Fotovoltaica: Cálculo de una instalación aislada, Second Edi. Barcelona, España: Marcombo, S.A, p. 200.
- N. Mohan (2010). Electrónica de Potencia, Convertidores, aplicaciones y diseño., 3^a. ed. Monterrey, Mexico: McGraw Hill, pp. 176–191.
- O. Style (2012). Energía solar autónoma, Oliver style. E.U: Paperback, p. 50.
- R. Cerrano (2013). Hacia una matriz energética diversificada en Ecuador. p. 42.
- R. Correa (2013). “Plan Nacional para el Buen Vivir 2009 – 2013, Estrategias para el Buen Vivir, Estrategia 7, Cambio de la Matriz Energética” <http://plan.senplades.gob.ec/estrategia7>.

R. Teodorescu (2011). Grid Converters for Photovoltaic and Wind Power Systems. New Delhi, India, p. 416.

S. Ang (2005). Power-Switching Converters, second edition. E.U: CRC Press, p. 18.

Ultracell (2013). “Batería 12V 150Ah Ultracell UCG 150-12 AGM Ciclo Profundo,” [Online]. Available: <http://www.digishop.cl/index.php?a=851>.